

SAT-1.307-1-MME-04

---

## CHANGES IN THE STRUCTURE DURING LASER TREATMENT OF AUSTENITIC STEEL

---

**Emil Yankov, Chief Assist. Prof., PhD**

Department of Material Science and Technology, University of Ruse “Angel Kanchev”, Bulgaria, E-mail: eyankov@uni-ruse.bg

**Maria Nikolova, Chief Assist. Prof., PhD**

Department of Material Science and Technology, University of Ruse “Angel Kanchev”, Bulgaria, E-mail: mpnikolova@uni-ruse.bg

**Vanya Zaharieva, Chief Assist. Prof., PhD**

Department of Material Science and Technology, University of Ruse “Angel Kanchev”, Bulgaria, E-mail: vzaharieva@uni-ruse.bg

**Marian Firov, Eng.**

ET “Deyan Madjarov – Madlock”, Ruse, Bulgaria,  
E-mail: office@madlock.net

***Abstract:** The advanced methods for treatment of materials with concentrated energy fluxes provide major opportunity for obtaining wear, fatigue, corrosion resistant and hard surfaces or persistently engraved ones with bitmaps in the form of texts or images. Today, we are aware of many methods of treatment but the laser technology is known to be highly accurate in positioning. In this respect, the laser treatment together with additionally applied combustible particulate substances (like magnesium paste, black powder, REX-C100-C900, etc.) on the treated surface enables obtaining of enhanced tribological properties while guaranteeing a certain depth of the treatment.*

*The present study aims at determining a regime for obtaining lasting traces with fiber laser for decorative purposes on an austenitic AISI 301 sheet steel. The result of the applied treatment is evaluated by means of microstructure, XRD analysis and tribological examinations. They show that the use of the concentrated power-controlled light beam that transmits the energy to the active magnesium paste produces qualitative and process-controlled surface treatments.*

***Keywords:** Fiber laser, Magnesium paste, Concentrated energy fluxes, High speed surface marking, Microstructure, XDR, Tribology, Hardness.*

### I. INTRODUCTION

In the modern mechanical engineering the surface treatment of materials is achieved by using concentrated energy fluxes that provides the opportunity of receiving products conforming of well-defined operation parameters and properties. One way of the technology of materials applies concentrated plasma, electron beam, electric arc or laser sources for surface treatment in engineering practice [1]. Some of these methods require the use of expensive equipment, large local installations or keeping specific conditions to receive the treated surface.

The laser treatment is identified with controlled surface area of thermal influence that leads to small gradient zones of phase transformations, as well as opportunities for precise positioning in length and width. The laser treatment over the recent years becomes more accessible with the production of small size installations at lower cost and lower energy intensity. Another advantage of this method is that the speed of the treatment could vary widely [2, 3].

The present study is directed towards a surface treatment of austenitic steel with modern optical fiber laser in order to identify the process parameters as regards obtaining mechanically durable, lasting heat treated surface. In order to reduce the energy consumption for the treatment and to make the impact zone small but effective, additionally added combustible particulate substance – magnesium (Mg) paste is used. The latter enables the cost of the ultrafast treatment by

the concentrated energy flux to become lower. Such examinations raised in the available scientific literature are not known at present.

## II. EXPERIMENTAL PROCEDURES

### 2.1. Materials, samples preparation and fiber laser treatment

The choice of the material is prompted by the broad applicability of the austenitic steels, the lower thermal conductivity of the material and the higher labor intensity for treatment with concentrated energy fluxes. Metal alloy X10CrNi18-8 (AISI 301, DIN 1.4310) in the form of 1.5 mm thick sheet with chemical composition (on the basis of the alloy specification) shown in Table 1 was used for the experiments. Square samples with dimensions 30×30 mm were cut out from the sheet metal and used to determine the main parameters of the laser treating regime. After the specification of these parameters, the experimental sampling regime was chosen and shown in Table 2.

Table 1. Chemical composition of X10CrNi18-8 steel.

Element	C	Si	Mn	Cr	Ni	Mo	S	P	N	Fe
Wt. %	< 0.12	< 0.75	< 2.00	16.0-18.0	6.0-8.0	-	< 0.03	< 0.04	< 0.1	Bal.

Table 2. Processing parameters of the chosen fiber laser treatment.

Material	Main parameters of the laser treating regime				
	Rate	Working gas pressure	Working gas	Laser power	Focal distance
	mm/min	m/bar	-	W	mm
X10CrNi18-8	5000	600	O <sub>2</sub>	120	-1.5

The laser treatment was conducted by NUKON Fiber Laser-1530 machine with a power of less than 2 kW. In order to achieve the objective of reducing the laser beam dwelling time and the depth of the heat treated zone, on the preliminary prepared and cleaned surface evenly spread magnesium paste was placed.

### 2.2. Characterization techniques

The light optical microscopy was performed on the top surface of the samples using a Nikon microscope without etching the samples. To ensure the comparability of the survey results for all samples one and the same magnification was utilized. The 14-megapixel digital camera was adapted to the microscope and used for the image acquisition.

A Vickers Hardness tester 432 SVD by Wilson-Wilpert was used for the hardness measurements of the steel according to the standard EN ISO 6507-1:2006 [4]. In order to compare the hardness changes the researches were made on the top view of each sample with a load of 0.3 kg and 5 kg and dwell time of 10s. Ten sequential measurements by increments of at least 50 μm between the imprints were made. Consequently, the data received were gathered in tables for comparative analysis. The summary results of the hardness measurements were presented in graphical form.

The scratch tests were performed on the top surface of the sample with a CSM REVETEST Scratch Macrotester equipped with a Rockwell C diamond indenter of 200 μm radius. Progressive load scratching mode with normal force range of 0N to 50N and 0N to 100N was used in the experiments at a speed of 10 N/mm. The scratch track was evaluated using optical methods of localized regions of poor adhesion and failure for each scratch as well as by means of secondary digital-signal records of the coefficient of friction ( $\mu$ ) and tangential force ( $F_t$ ).

The X-ray phase identification was performed with URD-6 diffractometer, applying Bragg-Brentano geometry and FF Fe-K $\alpha$  radiation and working at U = 30 kV and I = 20 mA. The diffraction angle range scanned was 35-129° 2 $\theta$  with a step size of 0.1°2 $\theta$  and counting time of

5s/step. The qualitative phase analysis was held using Match!3 software. The texture analyses were performed by calculating the texture coefficient (TC) [5] measuring the relative degree, of preferential orientation among the crystal planes:

$$TC_{(hkl)} = \frac{\frac{I_{(hkl)}}{I_{0(hkl)}}}{\frac{1}{N} \sum \frac{I_{(hkl)}}{I_{0(hkl)}}}, \quad (1)$$

where  $I_{(hkl)}$  and  $I_{0(hkl)}$  are the measured intensity and standard integrated intensity for (hkl) reflection, respectively, and  $N$  is the number of reflections observed. The data are taken from the results process by the Match!3 software. A  $TC > 1$  indicates preferential orientation.

### III. RESULTS AND DISCUSSIONS

The austenitic steel material is supplied in the form of metal sheets with dimensions 100×500 mm. Before the examinations the sheets have been mechanically cleaned from the “skin pass” (“pinch pass”) effect and degreased in order to avoid negative consequences such as surface coloring. The material so treated surface is shown in Fig. 1a, where it could be clearly seen the tracks of the above described cleaning. That state of the surface is called “untreated” in the present study and used for the laser treatment and the other examinations.

After the laser treatment the surface contains traces of the consistent movements of the laser beam (Fig. 1b). Different zones of fast solidified surface could be observed. The black looking craters are traces of the laser pulses where the material crystallizes in the shape of drops while around these drops dendrite-like structures are seen because of the non-equilibrium crystallization.

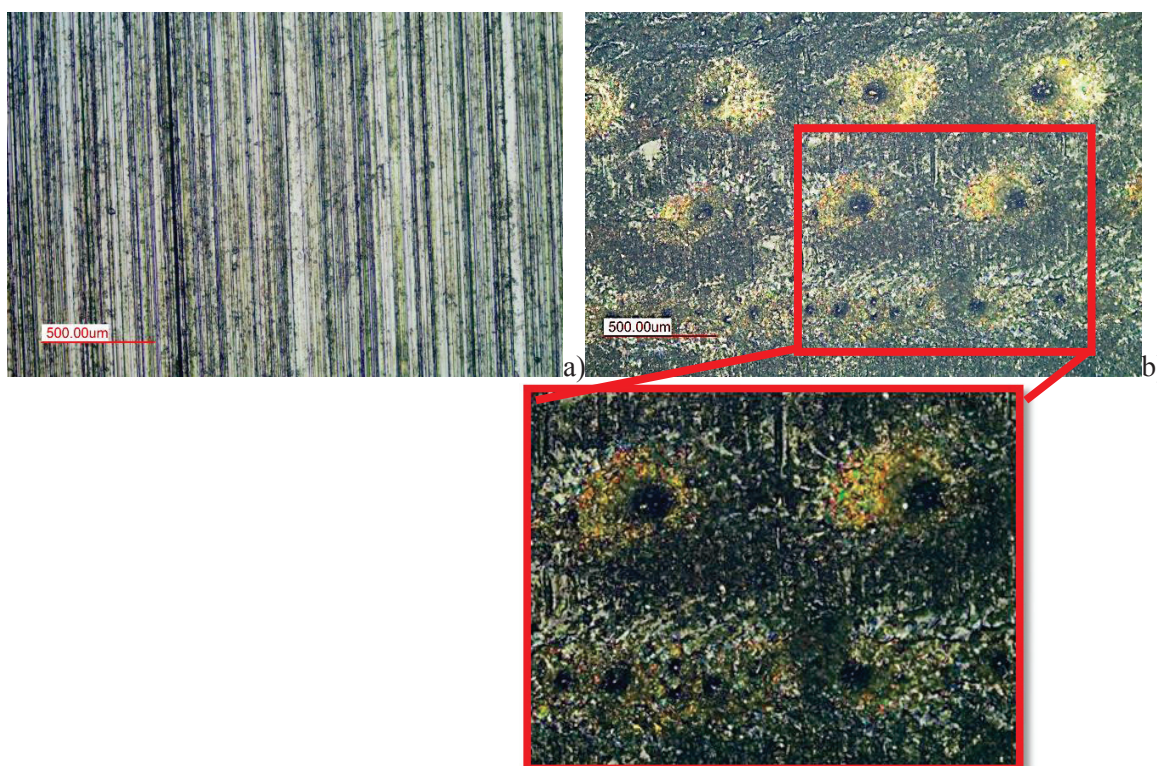


Fig. 1. Microstructure images of the surface of: a) untreated steel; b) laser treated with Mg paste austenitic steel.

The XRD analysis of the austenitic steel shows that the sheet material has been previously annealed because the 100% diffraction maximum  $(111)_\gamma$  possesses the highest intensity of all

detected austenitic peaks and all lines are sharp and high. Despite the thermal treatment the intensities of the  $(202)_\gamma$  and  $(311)_\gamma$  diffraction lines exceed over 2.5 times the theoretical values, indicating the presence of residual traces of preferred orientation (texture) from the previous technological processes. Further, except the metastable austenite phase (89.7%), within the untreated sheet materials weak  $\alpha'$ -lines (almost 10.3%) of low carbon martensite with tetragonal lattice are also detected (Fig. 2a).

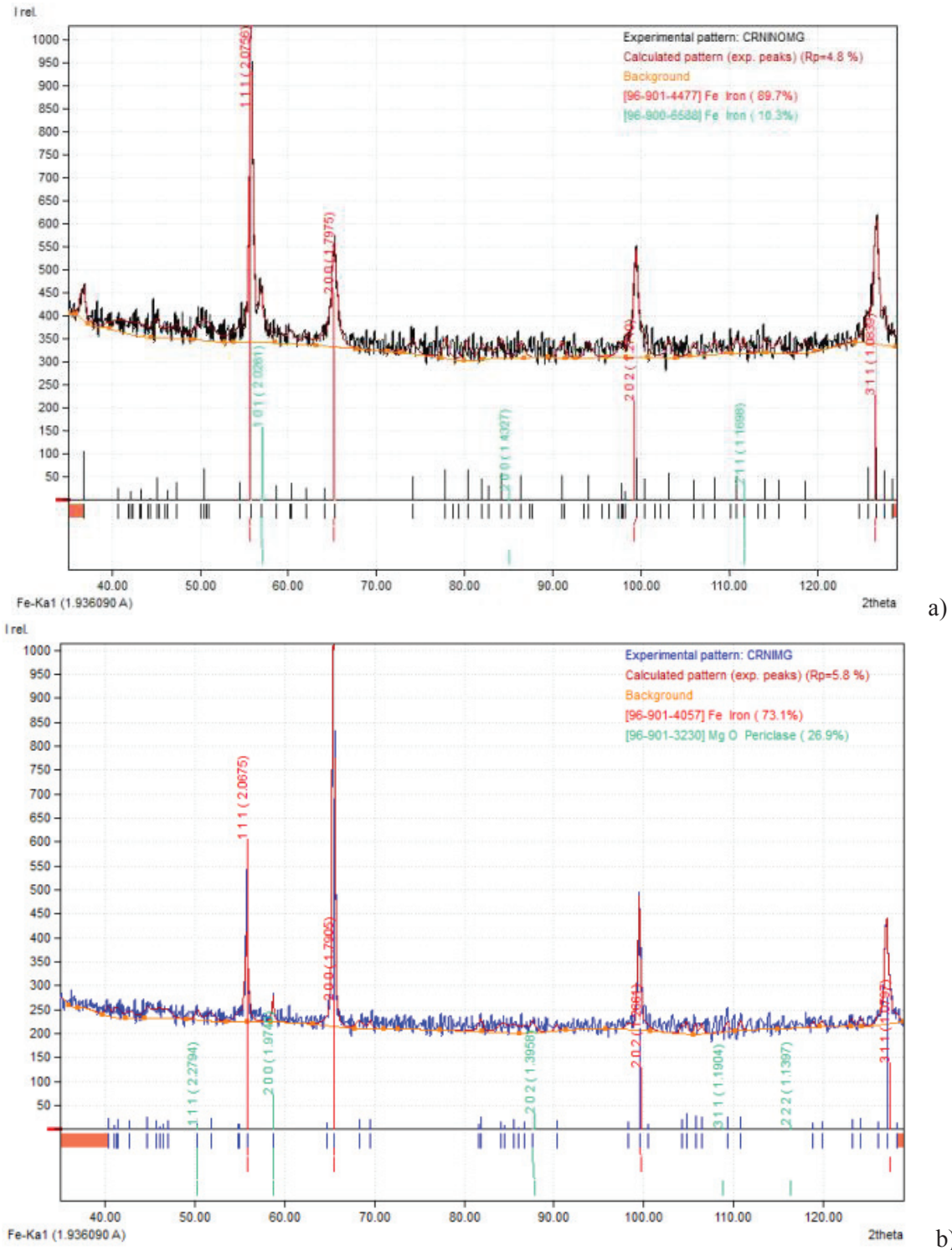


Fig. 2. Diffraction patterns of X10CrNi18-8 steel in the initial state (a) and after the laser treatment (b)

After the laser treatment with Mg paste the intensity of the austenitic  $(111)_\gamma$  line decreases with 45% while that of the  $(200)_\gamma$  plane increases with 73% (Fig. 2b). The observed changes in the

intensities highlight that the number of atoms present in  $(200)_\gamma$  plane increases because of the preferential growth in the particular direction. Therefore, particular changes in the degree of order of the crystals occur. The intensity of the other two peaks –  $(202)_\gamma$  and  $(311)_\gamma$  also decreases with 10% and 29.88%, respectively compared with the untreated sample planes that shows a weaker change in the structure of these planes (Fig. 3). Except the austenitic peaks in the laser treated sample weak reflections of MgO (green peaks with overall 26.9%) are also present (Fig. 2b).

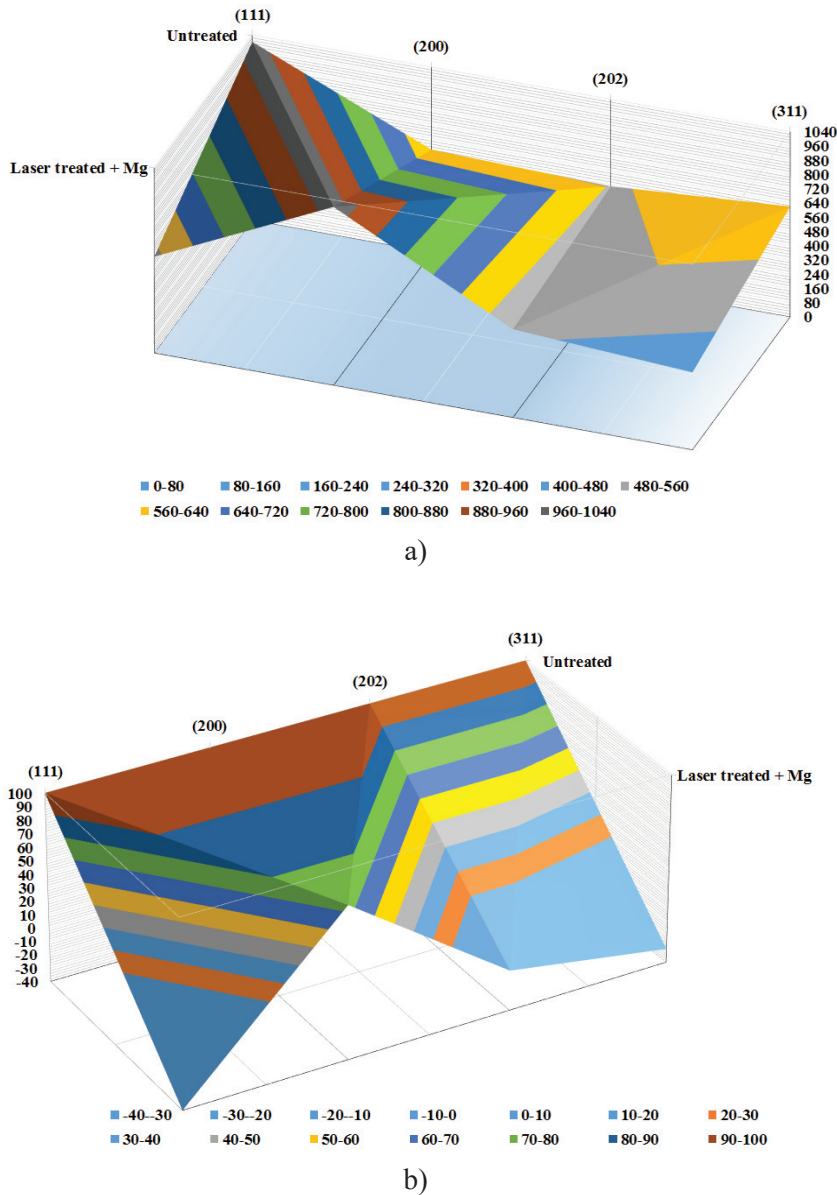


Fig. 3. Changes in the intensities, presented in 3D surface: a) absolute values of the intensities; b) relative change in the intensities of the laser treated compared with the untreated sample.

For reasons of comparability of the austenitic peaks position both XRD patterns are brought together and presented in Fig. 4. The austenite lines of the laser treated sample are shifted toward the higher angles with the exception of the closed packed  $(111)_\gamma$  plane where there is lack of such a shift. As a percentage applied to the untreated sample the  $(200)_\gamma$ ,  $(202)_\gamma$  and  $(311)_\gamma$  the shift is equal to 0.26%, 0.07% and 0.29%, respectively. The reason for the observed effect could be attributed to the increased crystal defects, deformations and changes in the degree of order in the crystals during the intensive non-equilibrium cooling down of the melted material and the resultant thermal stresses occurring near to the surface. As the solidification process is very sensitive to micro-porosities [6], such surface defects could also be expected.

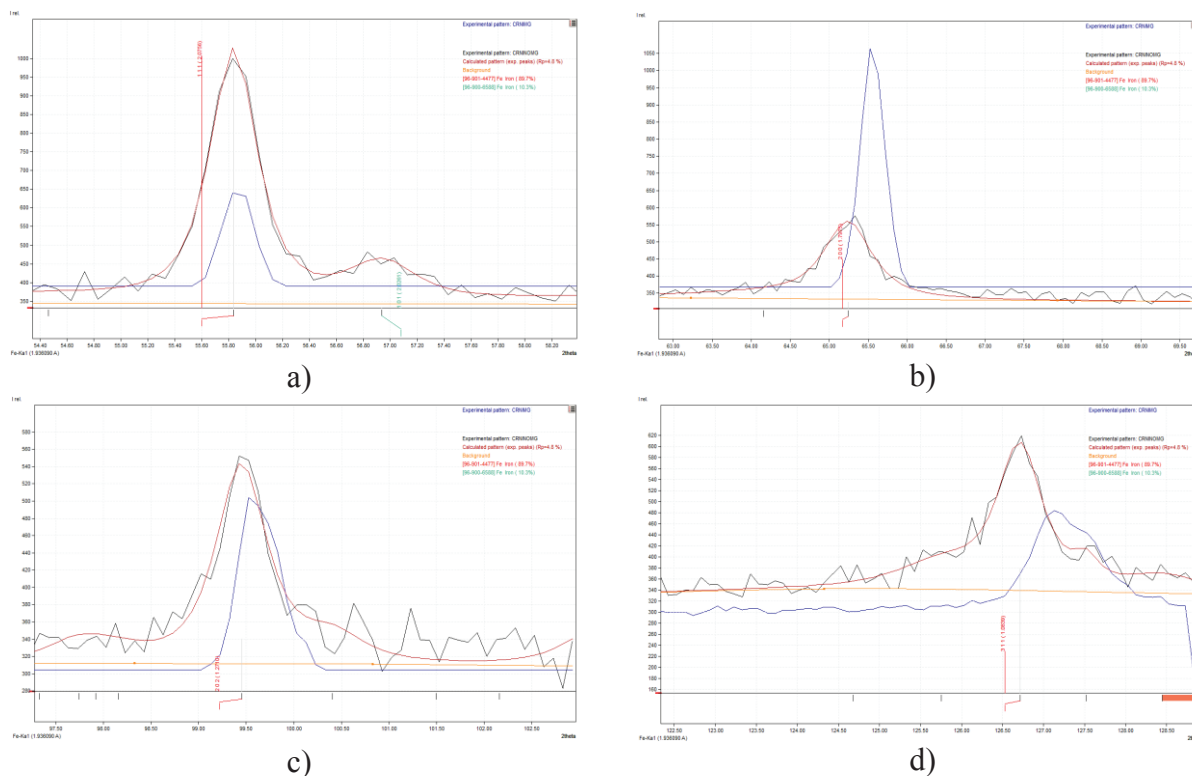


Fig. 4. Comparison of the austenite peaks of X10CrNi18-8 in untreated state and after the laser treatment of crystallographic planes: a)  $(111)_{\gamma}$ ; b)  $(200)_{\gamma}$ ; c)  $(202)_{\gamma}$ ; d)  $(311)_{\gamma}$ ;

After calculating the texture coefficients (Fig. 5) of the untreated samples the preferential orientation of the  $(202)_{\gamma}$  and  $(311)_{\gamma}$  is confirmed once again. The texture coefficient after the laser treatment with Mg paste increases in  $(200)_{\gamma}$  plane with above 100%, while in  $(202)_{\gamma}$  and  $(311)_{\gamma}$  planes slightly decreases (with 9.7 and 7.6 %, respectively). The decrease in the  $(111)_{\gamma}$  plane is the highest - over 50%. The results suggest that the non-equilibrium transformations during the fast heating and cooling down change the inherited texture. Because the XRD analysis is sensitive to the volume, the changes in the TC of the laser treated sample could be also attributed to the structure distortion and changes in the heat treated zone.

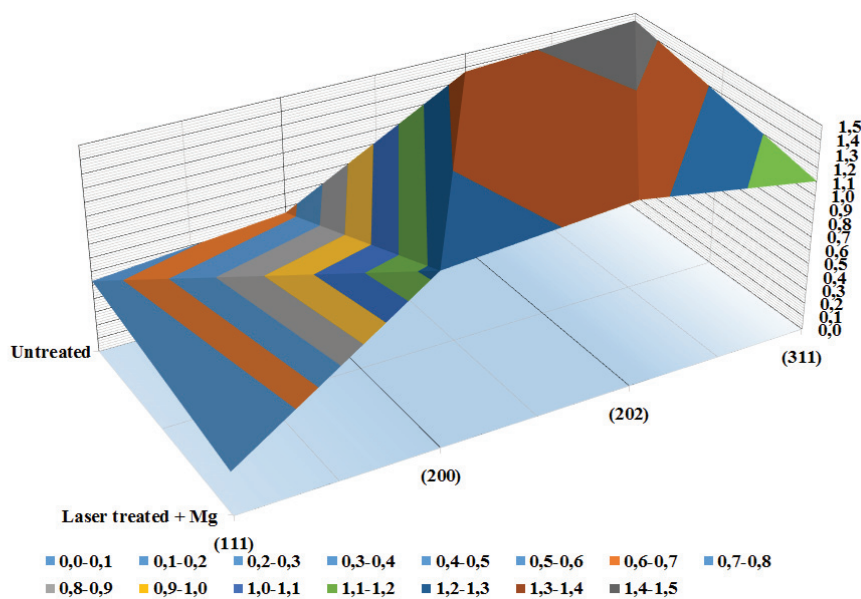


Fig. 5. Calculated absolute texture coefficients of the austenitic steel and the laser treated samples compared with the reference values of the crystallographic planes intensities and presented in 3D surface.

The established changes in the crystallographic planes provoked the performance of tribological tests for the examined surfaces. The measurements show that after the laser treatment with Mg paste the hardness values decrease with 12% when measured with a load of 300g (HV<sub>0.3</sub>) and slightly increase (with 1.5%) when the load becomes 5 kg (HV<sub>5</sub>). The main reason for this could be considered to be the difference in the surface and in-depth structures obtained after the laser treatment with the Mg paste.

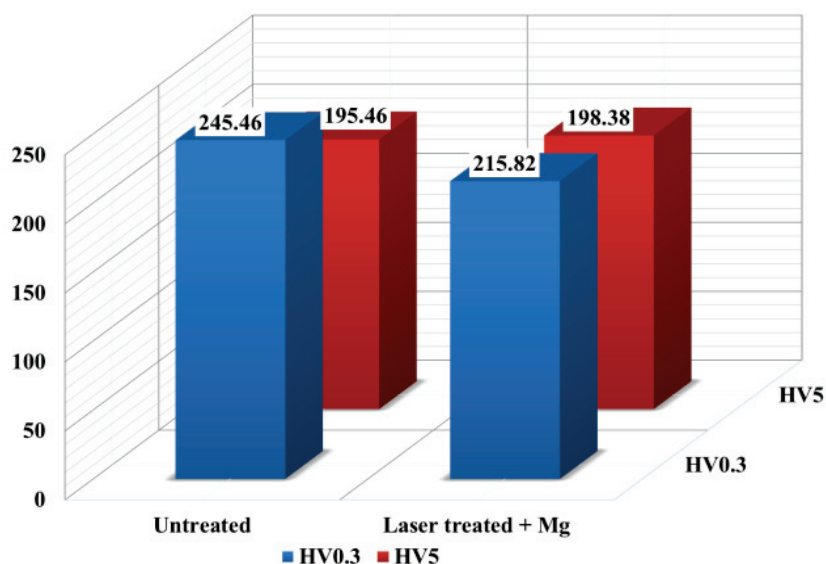


Fig. 6. Average hardness values before and after the laser treatment test measured at the top area of the samples.

In order to determine the durability of the laser treated surface a progressive load scratch test from 0 to 50N is carried out. The values of the coefficient of friction ( $\mu$ ) in the direction of the laser treatment ( $0^\circ$ ) of both untreated and laser treated samples present similarities. There are slight differences in the values during the initial state (small loading) where  $\mu$  shows a little bit higher values after the laser treatment that corresponds to the lower hardness values measured on the surface as well as the presence of MgO there. As the load increases,  $\mu$  values after the treatment become more uniform than that of the untreated austenitic steel. Because of the elastic response of the material the  $\mu$  values after the treatment rise up to over 0.45 while that of the untreated steel reach up to about 0.42 under 50N load. This effect could be related to the tangential force action, material resistance and the hardness values of the substrate.

Since the examined material is a sheet metal, the same examination is held at perpendicular direction in order to determine the influence of the texture on the scratch behavior (Fig. 8). The  $\mu$  values in the perpendicular direction of both samples demonstrate lower coefficient of friction in contrast to  $0^\circ$  tested ones. Deviations towards higher  $\mu$  values are observed in the untreated sample in this direction (Fig. 8). The width of the scratch track in this sample is also greater. With the increase in loading, both coefficients of the untreated and laser treated samples overlap and during the last test stage the  $\mu$  values show similar result of almost 0.45. This similarity could also be attributed to the equally acting tangential stresses in both cases and the similar material resistance.

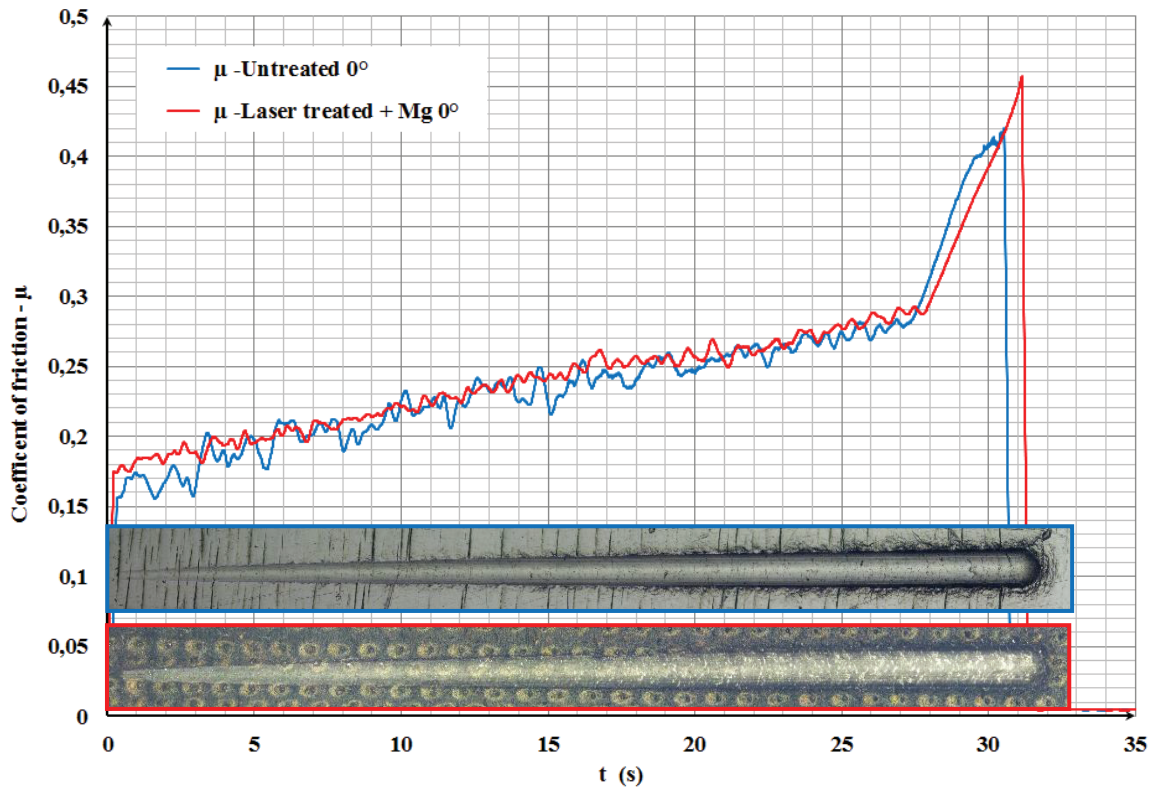


Fig. 7. Changes in the coefficient of friction ( $\mu$ ) from 0 to 50N normal force before and after the laser treatment test measured at the direction of the sample treatment.

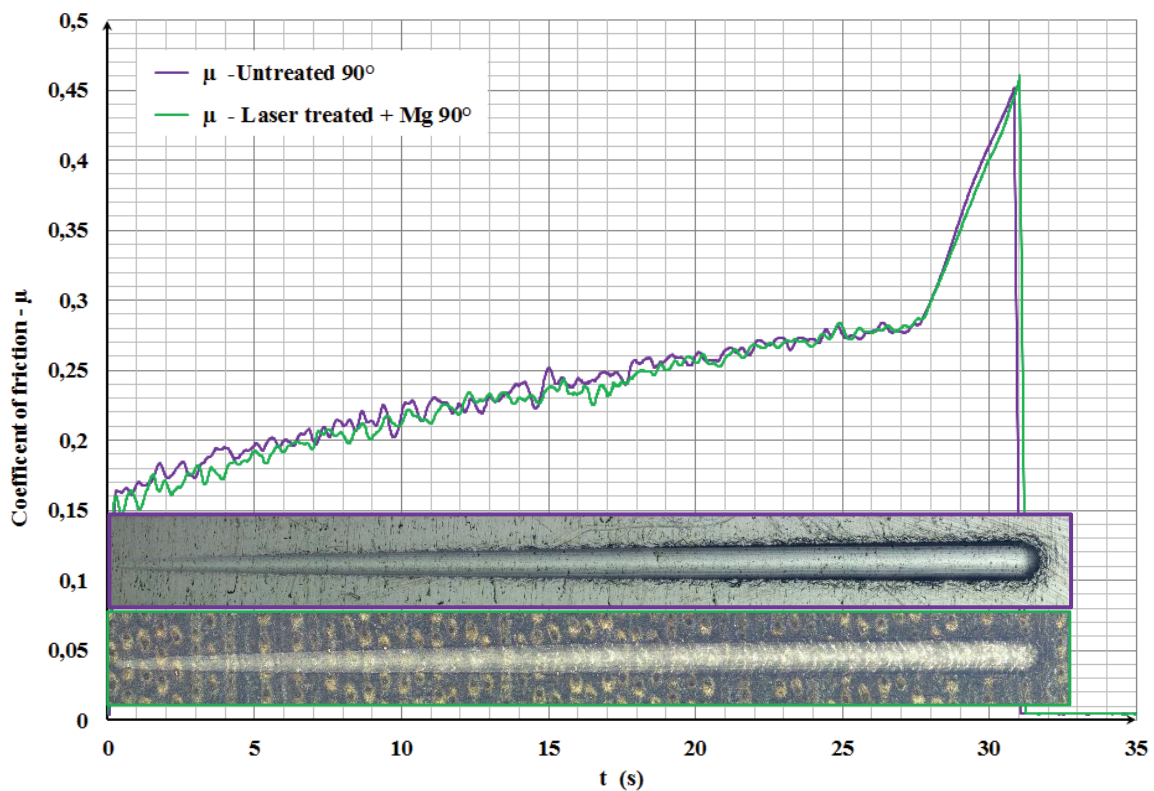


Fig. 8. Changes in the coefficient of friction ( $\mu$ ) from 0 to 50N normal force before and after the laser treatment test measured at the perpendicular direction of the sample treatment.

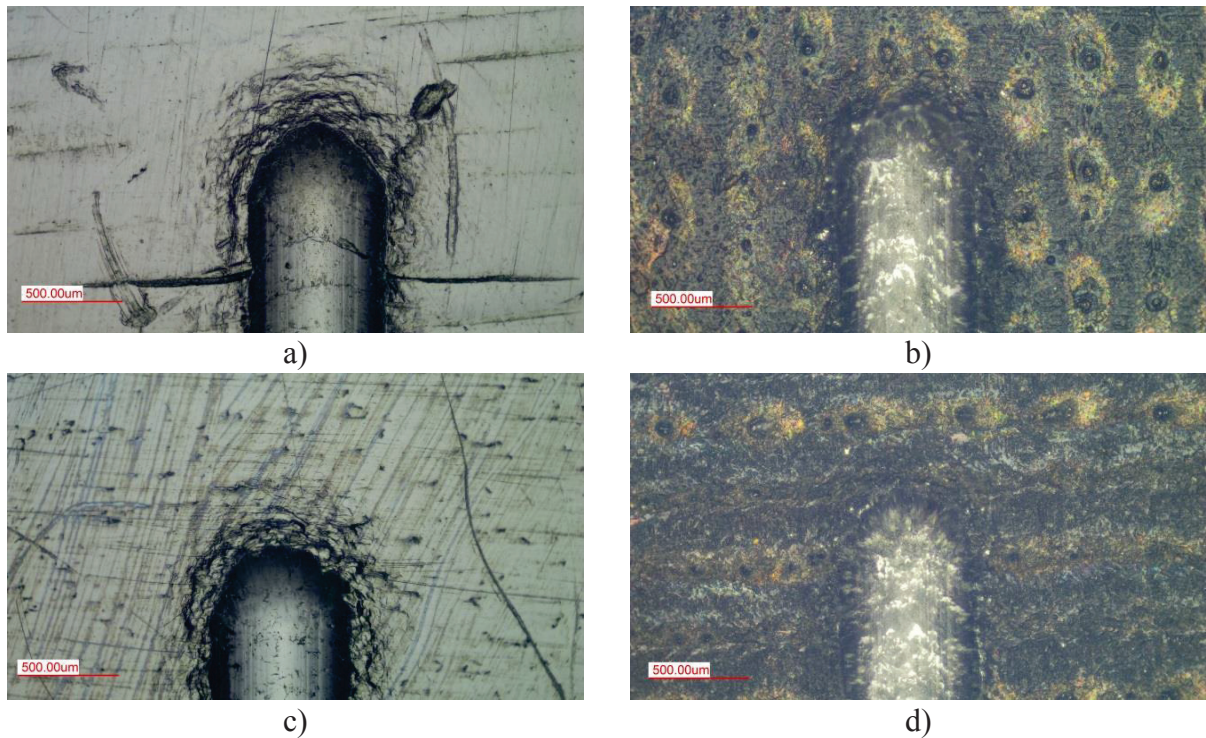


Fig. 9. Microstructure images at the end of the scratch tracks under 50N load of: a) untreated sample tested at the direction of the treatment; b) after the laser treatment measured at the direction of the treatment; c) untreated sample tested at the perpendicular direction of the sample treatment; d) laser treated measured at the perpendicular direction of the sample treatment.

Near the final loading stage differences in the structure of both samples (Fig. 9a and b) could be observed: comparatively coarse grained structure around the scratch truck of the untreated steel and more finely grained within the laser treated. Unlike the untreated steel, the limited fluctuations of the  $\mu$  values of the laser treated sample at the initial loading stage (Fig. 7) are further evidence for the surface grain refinement.

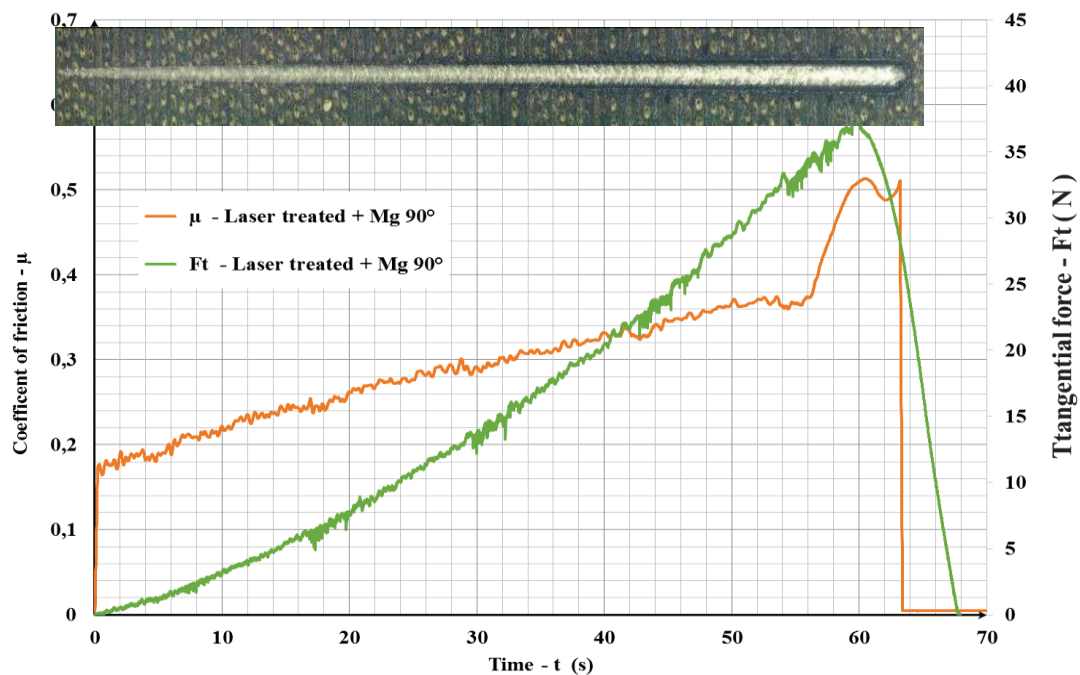


Fig. 10. Changes in the coefficient of friction ( $\mu$ ) and tangential force ( $F_t$ ) from 0 to 100 N normal force after the laser treatment test measured at the direction of the sample treatment.

The observed grain structure at the end of the scratch track in perpendicular direction (Fig. 9c) indicates that the material is mainly laterally shifted in contrast to the same sample tested in the longitudinal direction.

As seen from the scratch track images, a full penetration of the indenter towards the substrate of the laser treated sample at maximal load of 50 N is not observed. That's why a progressive scratching mode with normal force increasing up to 100 N is held for the laser treated sample. The results are shown in Fig. 10. When using 100 N maximal load clearly visible substrate areas are detected in the final 1/3 of the track. The  $\mu$  value curve has similar nature up to 50N as the previous scratch examinations of this sample and at the end it reaches maximal value of above 0.5. During stylus unloading the  $\mu$  curve acquires specific nature with slight decrease followed by an increase. This effect is probably due to the deeper penetration of the stylus and the adhered to the indenter substrate material. The  $F_t$  curve also has a similar nature to that registered up to 50N load. The maximum  $F_t$  values rise up to over 37N.

The tribological behavior of the examined material is also assessed by measuring the tangential force ( $F_t$ ) in both directions of both untreated and laser treated samples. The results shown in Fig. 11, illustrate that the untreated material possesses a higher loading resistance in both directions because the average  $F_t$  values are higher at the end of the examination (Fig. 11a, b). This has a time-shift effect in the  $F_t$  diagrams of both examined directions of the untreated sample. The laser treated surface shows a lower loading resistance in tangential direction than the untreated one.

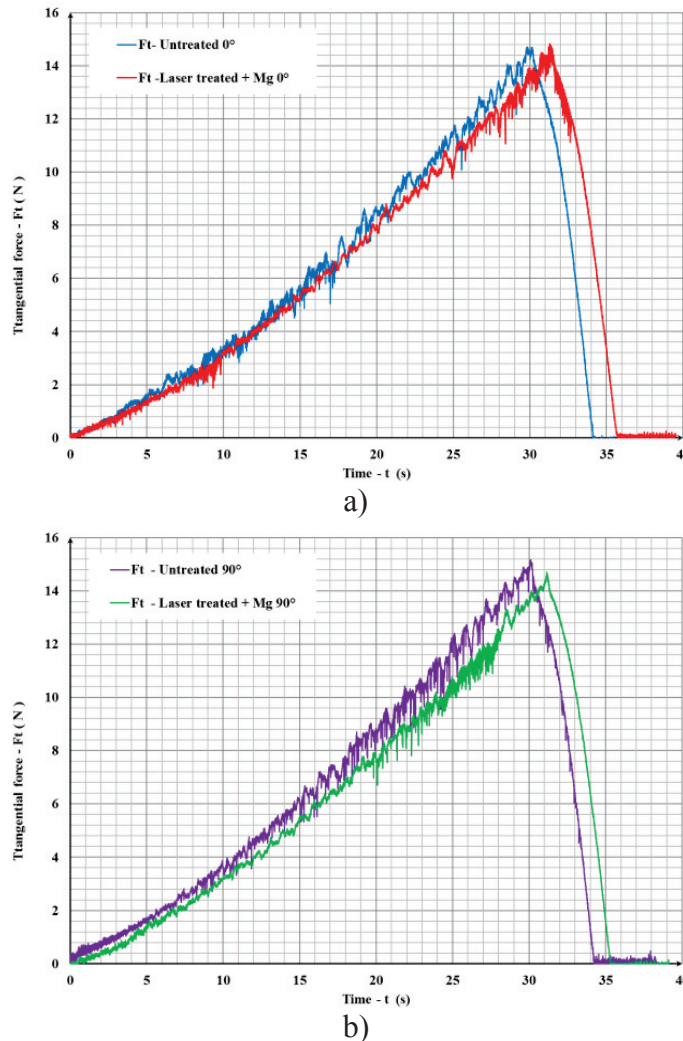


Fig. 11. Changes in the tangential force from 0 to 50N normal force before and after the laser treatment measured: a) at the direction of the sample treatment of both treated and untreated samples; b) in the perpendicular direction of the sample treatment of both treated and untreated samples;

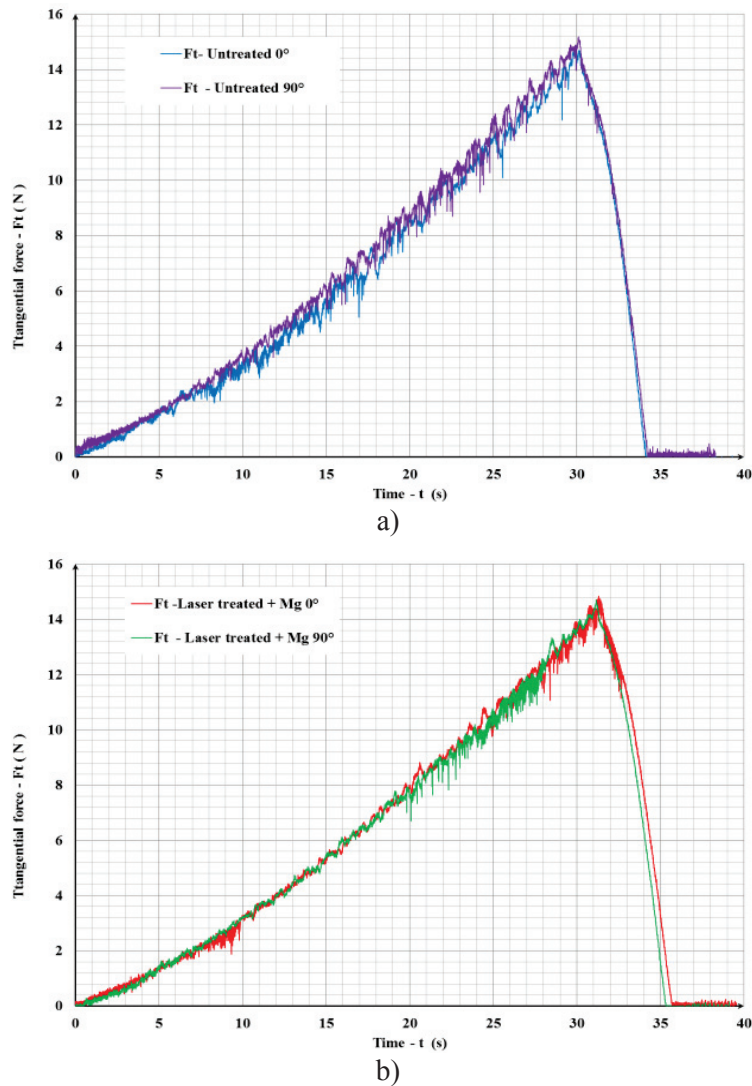


Fig. 12. Changes in the tangential force from 0 to 50N normal force before and after the laser treatment measured: a) at both directions of the untreated samples; b) at both directions of the treated samples.

The results from the data comparison of each sample tested in both directions (parallel and perpendicular to the treatment), Fig. 12a and b, confirm the previous examination results. In longitudinal direction of the untreated sample the  $F_t$  values show a lower trend than in the perpendicular direction (Fig. 12a). The changes occurring after the laser treatment lead to the structure homogenization and hardness decrease, because  $F_t$  value curves in both directions merely overlap (Fig. 12b).

#### IV. CONCLUSIONS

The use of laser together with Mg paste enables the production of a durable treated surface capable of withstanding a scratch normal load of over 50 N.

When using Mg paste after the crystallization of the melted zones a certain drop and dendrite-like non-equilibrium phases are seen on the laser treated surface. The austenitic steel substrate offers no possibility of hardness increase because of the low carbon content and the lack of solid state phase transformations that could give metastable hard products. The structural changes observed at the examined steel are only crystallographic reorientation that leads to the homogenization of the structure and properties in the near surface area. The inherited texture of the substrate material changes mainly at  $(200)_\gamma$  and  $(111)_\gamma$  planes after the treatment as the former intensity strongly increases and the later intensity decreases. Despite the increase in the texture

coefficient of the "hard" (200)<sub>γ</sub> plane, the measured hardness values before and after the treatment are similar because of the soft substrate and small thickness of the laser treated area.

The tribological analysis by means of scratch test shows that the coefficient of friction of the laser treated surface in both mutually perpendicular directions has similar character curves, while the  $\mu$  values are slightly higher for the untreated sample surface because of the inherited texture. This effect is confirmed by the lower  $F_t$  value curves for the laser treated surfaces. The proposed method for surface laser treatment could also be used for unification of the properties of the materials in the treated plane.

The presented study is a preliminary experiment that should be further developed by considering different regimes of laser treatments of the austenitic steel. Consequently, these regimes should be applied for different tool steels in order to examine the changes in the phase composition, structure and properties.

### **Acknowledgement**

The paper reflects the outcomes of the project № 16 – FMME – 02, financed by the Fund „Scientific Research” of University of Ruse “A. Kanchev”.

### **REFERENCES**

[1] Stavrev D., V. Shtarbakov, Ts. Dikova, Structure and Properties of Fe-C Alloys after Treatment with Concentrated Energy Fluxes, Edited by D. Stavrev, STENO, Varna, 2015, p. 294; ([https://www.researchgate.net/profile/Tsanka\\_Dikova/publication/281686055\\_STRUKTURA\\_I\\_SVOJSTVA\\_NA\\_ZELAZO-VGLERODNI\\_SPLAVI\\_SLED\\_VZDEJSTVIE\\_S\\_KONCETRIRANI\\_ENERGIJNI\\_POTOCI\\_STRUCTURE\\_AND\\_PROPERTIES\\_OF\\_Fe-C\\_ALLOYS\\_AFTER\\_TREATMENT\\_WITH\\_CONCENTRATED\\_ENERGY\\_FLUXES/links/55f473ab08ae6a-34f6608e68.pdf](https://www.researchgate.net/profile/Tsanka_Dikova/publication/281686055_STRUKTURA_I_SVOJSTVA_NA_ZELAZO-VGLERODNI_SPLAVI_SLED_VZDEJSTVIE_S_KONCETRIRANI_ENERGIJNI_POTOCI_STRUCTURE_AND_PROPERTIES_OF_Fe-C_ALLOYS_AFTER_TREATMENT_WITH_CONCENTRATED_ENERGY_FLUXES/links/55f473ab08ae6a-34f6608e68.pdf))

[2] [www.nukon.bg](http://www.nukon.bg);

[3] <http://www.trumpf-laser.com/en.html>;

[4] EN-ISO-6507-1:2006, ([http://www.bds-bg.org/bg/bg/standard/?natstandard\\_document\\_id=34645](http://www.bds-bg.org/bg/bg/standard/?natstandard_document_id=34645))

[5] Class26\_handout MTSE 3010 2013 Supplemental Texture & Grain Size Calculation.pdf, Polycrystallography, Institute of North Texas, 2013, [http://engineering.unt.edu/materials/sites/default/files/sites/default/files/lamma/oldsite/documents/Class26\\_handout%20MTSE%203010%202013%20SUPPLEMENTAL%20TEXTURE%20%26%20GRAIN%20SIZE%20CALCULATION.pdf](http://engineering.unt.edu/materials/sites/default/files/sites/default/files/lamma/oldsite/documents/Class26_handout%20MTSE%203010%202013%20SUPPLEMENTAL%20TEXTURE%20%26%20GRAIN%20SIZE%20CALCULATION.pdf);

[6] Henderieckx Ir G., B.V. Gietch, Solidification Mechanism Ductile Iron, April 2008, ([https://webcache.googleusercontent.com/search?q=cache:JpGSsvfeX\\_cJ:https://www.researchgate.net/file.PostFileLoader.html%3Fid%3D57ed7d1adc332dfe8628b7c4%26assetKey%3DAS%253A411756678664192%25401475181850343+&cd=1&hl=bg&ct=clnk&gl=bg](https://webcache.googleusercontent.com/search?q=cache:JpGSsvfeX_cJ:https://www.researchgate.net/file.PostFileLoader.html%3Fid%3D57ed7d1adc332dfe8628b7c4%26assetKey%3DAS%253A411756678664192%25401475181850343+&cd=1&hl=bg&ct=clnk&gl=bg));